Cancer Immunology, Immunotherapy (2019) 68:1573–1583
https://doi.org/10.1007/s00262-019-02390-0

ORIGINAL ARTICLE

Desmoid tumors display a strong immune infiltration at the tumor margins and no PD-L1-driven immune suppression

Vasiliki Siozopoulou[1,2] · Elly Marcq[1] · Julie Jacobs[1,2] · Karen Zwaenepoel[1,2] · Christophe Hermans[1,2] · Jantine Brauns[1,2] · Siegrid Pauwels[2] · Clément Huysentruyt[3] · Martin Lammens[2] · Johan Somville[4] · Evelien Smits[1,5] · Patrick Pauwels[1,2]

Received: 27 March 2019 / Accepted: 1 September 2019 / Published online: 11 September 2019

Abstract

Desmoid tumors (DTs) are local aggressive neoplasms, whose therapeutic approach has remained so far unsolved and in many instances controversial. Nowadays, immunotherapy appears to play a leading role in the treatment of various tumor types. Characterization of the tumor immune microenvironment (TME) and immune checkpoints can possibly help identify new immunotherapeutic targets for DTs. We performed immunohistochemistry (IHC) on 33 formalin-fixed paraffin-embedded (FFPE) tissue sections from DT samples to characterize the TME and the immune checkpoint expression profile. We stained for CD3, CD4, CD8, CD20, FoxP3, CD45RO, CD56, CD68, NKp46, granzyme B, CD27, CD70, PD1 and PD-L1. We investigated the expression of the markers in the tumoral stroma, as well as at the periphery of the tumor. We found that most of the tumors showed organization of lymphocytes into lymphoid aggregates at the periphery of the tumor, strongly resembling tertiary lymphoid organs (TLOs). The tumor expressed a significant number of memory T cells, both at the periphery and in the tumoral stroma. In the lymphoid aggregates, we also recognized a significant proportion of regulatory T cells. The immune checkpoint ligand PD-L1 was negative on the tumor cells in almost all samples. On the other hand, PD1 was partially expressed in lymphocytes at the periphery of the tumor. To conclude, we are the first to show that DTs display a strong immune infiltration at the tumor margins, with formation of lymphoid aggregates. Moreover, we demonstrated that there is no PD-L1-driven immune suppression present in the tumor cells.

Keywords Desmoid tumors · PD-L1 · Immunotherapy · Immunohistochemistry

Abbreviations

CTLA-4	Cytotoxic T lymphocyte antigen-4
DT	Desmoid tumors
FAP	Familial adenomatous polyposis
FFPE	Formalin-fixed paraffin embedded
HEV	High endothelial venules
HRMA	High-resolution melting analysis
IHC	Immunohistochemistry
LN	Lymph node
NGS	Next-generation sequencing
PD(L)-1	Programmed death (ligand)-1
RTU	Ready-to-use
Treg	Regulatory T cells
TLO	Tertiary lymphoid organs
TME	Tumor microenvironment

Electronic supplementary material The online version of this article (https://doi.org/10.1007/s00262-019-02390-0) contains supplementary material, which is available to authorized users.

✉ Vasiliki Siozopoulou
vasiliki.siozopoulou@uza.be

[1] Center for Oncological Research, University of Antwerp, Antwerp, Belgium

[2] Department of Pathology, Antwerp University Hospital, Wilrijkstraat 10, Edegem, 2650 Antwerp, Belgium

[3] PAMM Laboratory for Pathology and Medical Microbiology, Catharina Hospital, Eindhoven, The Netherlands

[4] Department of Orthopedic Surgery, Antwerp University Hospital, Antwerp, Belgium

[5] Center for Cell Therapy and Regenerative Medicine, Antwerp University Hospital, Antwerp, Belgium

Introduction

Desmoid tumors (DTs), also known as aggressive fibromatosis, represent a monoclonal proliferation of myofibroblasts arising from the musculoaponeurotic stromal element, which can develop at virtually any anatomic site. According to the newest WHO classification of soft tissue and bone tumors, DTs are neoplasms of intermediate malignant potential (locally aggressive) characterized by an infiltrative growth pattern into the surrounding normal structures, sometimes in a disruptive manner, but with no metastatic potential [1]. Nevertheless, they can be lethal for the patient due to destruction of vital tissues.

Morphologically, the tumor is composed of bland small, slender spindle cells without distinctive cytoplasmic borders. This tumor type is morphologically rather bland, since there is no nuclear pleomorphism, mitotic activity or necrosis. The aggressiveness of DTs has been proven by the infiltrative character of the neoplastic cells which invade and entrap the surrounding normal structures, with imminent risk when growing next to large vessels or other vital organs.

Many things about the pathogenesis of these tumors still remain unknown. The majority of DTs are sporadic, sometimes described after local trauma, pregnancy or injury [2–4]. In a recent study, 85% of DTs have shown somatic mutations of the beta catenin gene, CTNNB1 [3]. They can also develop as part of hereditary diseases, like familial adenomatous polyposis (FAP) syndrome. In FAP, a germline mutation involving the APC gene is the causative agent of the disease [2, 4, 5]. DTs associated with FAP syndrome, also referred to as the Gardner syndrome [7], have a predilection for abdominal localization and patients with FAP show an 80% risk for developing DTs. Both the CTNNB1 and APC genes are part of the Wnt signaling pathway [2]. Mutation of those genes can result in upregulation of β-catenin and accumulation into the nucleus where it activates Wnt pathway transcription factors [5]. Accordingly, nuclear positivity for β-catenin is an important diagnostic tool in the armamentarium of the soft tissue pathologist. Nuclear staining with immunohistochemistry (IHC) is reported in nearly 67–80% of cases [2, 6]. Given the rarity of this tumor and its ability to appear anywhere in the body, the therapeutic approaches are broad. Depending on the localization of the lesion and the overall condition of the patient, different treatment options are described, ranging from surgery to chemotherapy and radiotherapy [7]. However, in many instances the tumor recurs more aggressively after treatment. Therefore, the most preferable option for stable and asymptomatic disease is close monitoring of the patient, also called "watchful waiting" [2, 8]. Since treatment of DTs still remains challenging and due to its potential aggressive behavior, novel therapeutic strategies are required.

Over the past years, immunotherapy gained more and more interest among the therapeutic options for cancer treatment. Immunomodulation refers to the recruitment and activation of innate and adaptive immune cells to control the tumor growth and its metastatic potential. More recently, blockade of the immune checkpoints, cytotoxic T lymphocyte antigen-4 (CTLA-4) and programmed death-1 (PD1), has proven to be effective in the treatment of different tumor types, such as metastatic melanoma and renal cell carcinoma [9, 10]. Given the advantages of immunotherapy in other solid tumors, sarcomas might also be a good candidate. To date, there are few randomized trials and small studies about immunotherapy in sarcomas, including osteosarcoma, synovial sarcoma and rhabdomyosarcoma (reviewed ref [11]). However, surgery for localized tumors and cytotoxic therapy for more advanced diseases remain first-line treatment for soft tissue and bone tumors. To identify new therapeutic targets for soft tissue tumors, we characterized the immune cell composition of DT tissue samples and looked at the expression of immune checkpoints in the tumor microenvironment (TME) using IHC (Fig. 1).

Materials and methods

Patient selection and samples

Thirty-three (33) formalin-fixed paraffin-embedded (FFPE) archival tissue samples from 27 different patients with DTs were collected. Thirty (30) of those samples were retrieved from the Department of Pathology at the Antwerp University Hospital and they were collected between 2009 and 2016. Three (3) other samples were kindly provided by the Laboratory for Pathology and Medical Microbiology (PAMM) at the Catharina Hospital in Eindhoven, collected in 2015. Twenty-four (24) of the 33 samples were excision specimens, while the other 9 samples were biopsy material (Supplementary Fig. 1). The biopsy samples were fixed in 4% formaldehyde for up to 12 h, while the excision samples were fixed for up to 32 h and paraffin embedded on a routine basis.

Immunohistochemistry

Five-µm-thick sections were prepared from FFPE tissue blocks and baked in an oven for 2 h at 60 °C prior to staining. Following IHC, stainings were performed on a Benchmark Ultra XT autostainer (Ventana Medical Systems Inc, Roche) according to the manufacturer's datasheets: anti-CD3 (clone 2GV6, ready-to-use (RTU), Ventana, anti-CD4 (clone SP35, RTU, Ventana), anti-CD8 (clone SP57, RTU, Ventana), anti-PD1 (clone NAT105, RTU, Ventana) and anti-CD45RO (clone UCHL-1, RTU, Ventana).

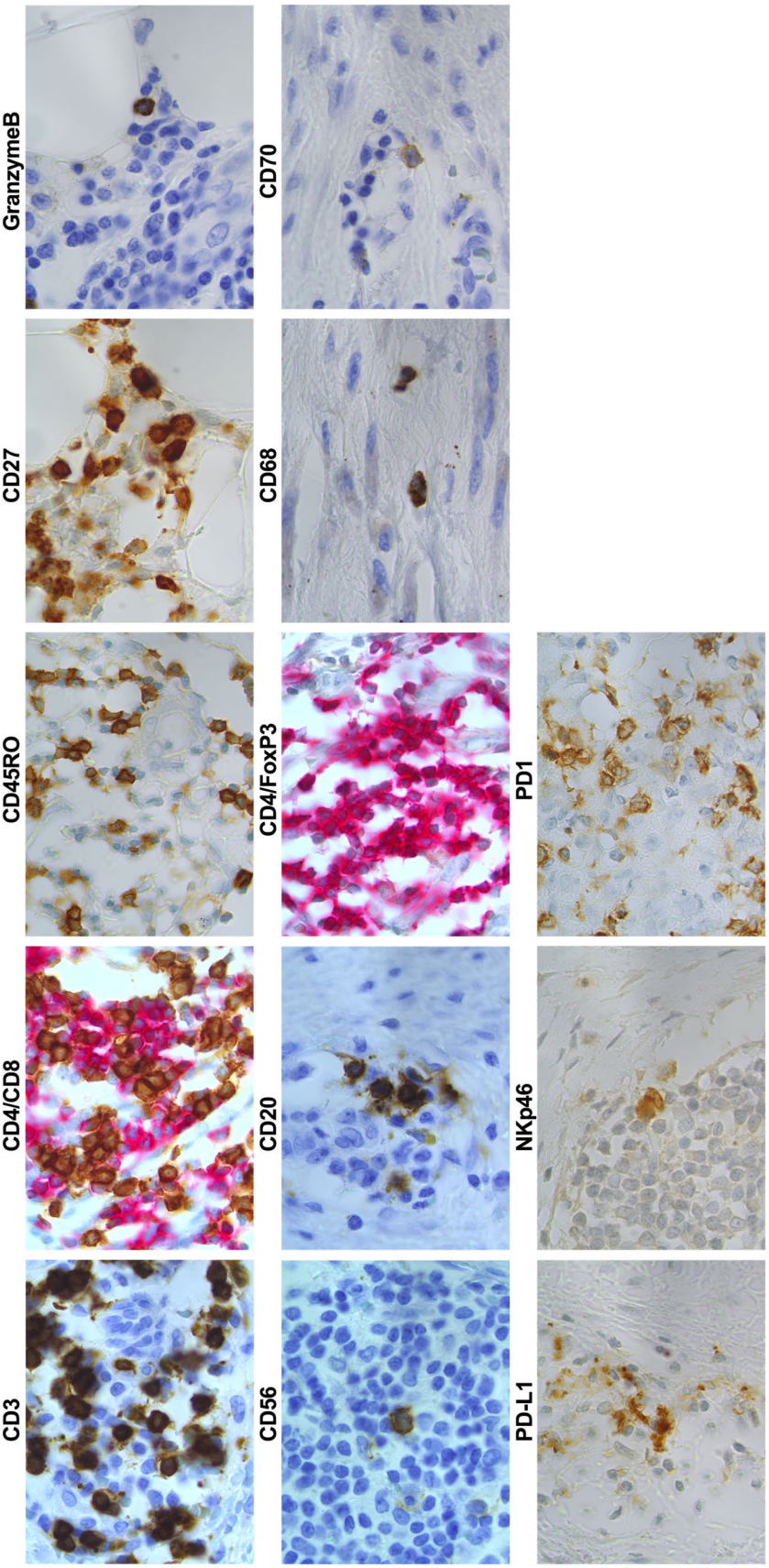

Fig. 1 Representative immunohistochemical staining patterns of different immunomarkers in DT tissue samples. Dual staining was used for CD4 (red, cytoplasmic)/CD8 (brown, cytoplasmic) as well as for CD4 (red, cytoplasmic)/FoxP3 (brown, nuclear). All tissue sections were counterstained with hematoxylin (blue color). Original magnification ×1000

The FOXP3, PD-L1, CD27 and NKp46 IHC were also performed on the Benchmark Ultra XT with a protocol that was slightly adapted from the datasheet: anti-FoxP3 (clone 236A/E7, 1/50 for 40 min, Abcam) in combination with a mild pretreatment with CC1 and the UltraView detection kit, anti-PD-L1 (clone E1L3 N 1/150 for 44 min, Cell Signaling Technologies) in combination with a mild pretreatment with CC1 and the OptiView detection and Amplification kit, anti-NKp46 (clone 195314, 1/50 for 40 min, R&D systems) in combination with mild CC1 pretreatment and UltraView detection, anti-CD27 (clone 137B4, 1/25 for 40 min, Thermo Fisher Scientific) in combination with a mild CC1 pretreatment and the OptiView detection and OptiView Amplification kit. The CD68, B catenin 1, CD20, CD56 and granzyme B IHC were performed on a Dako Omnis instrument (Agilent) in combination with the Envision Flex detection system (Agilent) with minor alterations to the manufacturer's datasheet: anti-CD68 (clone KP-1, RTU for 25 min, Dako), anti-granzyme B (clone GrB-7 1./50 for 32 min, Dako), anti-CD20 (clone L26, RTU for 12.5 min, DAKO), anti-CD56 (clone 123C3, RTU for 30 min, Dako) and anti-beta catenin (clone beta-catenin-1, RTU for 22.5 min, Dako).

CD70 IHC was performed on the Dako PT Link and Autostainer Link using the anti-CD70 (CD27 Ligand, Clone 301731, 1/40 for 20 min, R&D systems) as described by Jacobs et al. [12].

Upon staining, the sections were counterstained with hematoxylin as part of the automated staining protocol. After staining, slides were washed in reaction buffer (Ventana), dehydrated in graded alcohol, cleared in xylene, mounted with Quick-D Mounting Medium (Klinipath) and coverslipped.

Positive controls were included in each staining and consisted of tonsil tissue or placenta tissue (specifically for PDL-1). All stained slides were assessed and scored independently by two pathologists and one scientist, as described by Marcq et al. [13]. We looked at the presence of tumor infiltrating lymphocytes and lymphoid aggregates (score 0 = 0 aggregates; 1 = 1–5 aggregates; 2 = 5–10 aggregates; 3 = > 10 aggregates). Expression of each marker in the tissue was divided into five categories (0 = < 1%; 1 = 1–< 5%; 2 = 5–< 10%; 3 = 10–< 50%: 4 = ≥ 50%). A cutoff value of ≥ 1% was used to determine the positivity of all samples. Samples were considered to be positive in case of > 1% positive cells, with specific staining of any intensity (0 = no expression, 1 = weak, 2 = moderate, 3 = strong) and any distribution (membrane and/or cytoplasm). These criteria were used for IHC scoring of all the different markers [13]. An Olympus BX41 microscope was used for scoring of the tissue sections. Pictures were made using the Leica acquisition software v4.

Molecular test

For CTNNB1 mutation analysis, DNA was extracted from FFPE tissue blocks using the QIAmp DNA FFPE tissue kit (Qiagen), according to the manufacturer's instructions. CTNNB1 mutations in exon 3 were investigated using high-resolution melting analysis (HRMA) on a lightCycler 480 instrument (Roche Diagnostics Gmbh), using the following primers: 5′-GTAAAACGACGGCCAGAGTCACTGGCA GCAACAGT C-3′ and 5′-AGCGGATAACAATTTCAC ACAGGTCTTCCTCAGGATTGCCTT-3′. High-resolution melt analysis (HRMA was assessed using GeneScanning software (Roche). HRMA products with a deviating CTNNB melting pattern were directly purified using ExoSAP-IT (Affymetrix) and the purified PCR product was used as template for direct Sanger sequencing (Big Dye Terminator v1.1 kit (Applied Biosystems) using M13 tag primers (Eurogentec, Seraing, Belgium) on a 3130 XL Genetic Analyzer (Applied Biosystems)). Sequencing data were analyzed using SeqScanner software (Applied Biosystems).

The material harboring a mutation was further analyzed with next-generation sequencing (NGS) to retrieve the mutation status of the tumors. Next-generation sequencing was performed using a HaloPlex custom panel (Agilent) on a MiSeq instrument (Illumina). Variant analysis was performed using SeqNext software (JSI).

Statistics

Associations of immunological markers, such as CD3, CD4 and CD20, with clinicopathological parameters of DT patients were investigated by χ^2 analysis or Fisher's exact test (when appropriate). Spearman correlation coefficients (R) were calculated to investigate the correlation between the expression of immunological markers within DT specimens. All analyses were performed using SPSS version 23 and significance was reached if $P < 0.05$ (two-tailed).

Results

Patient characteristics

The clinicopathological characteristics of our patient cohort are summarized in Table 1. Thirty-three samples from 27 different patients were included in this study. Within our patient cohort, there was a slight female predominance with a female/male ratio of almost 1.5/1. The age at the time of the initial diagnosis ranged from 18 to 70 years with a median of 44.8 years.

Almost half of the patients (13/27) had a tumor that was located intra-abdominally (abdomen and mediastinum). Some of the tumors seem to have occurred after

Table 1 Clinicopathological parameters

Characteristics	*N*
Age (years)	
Median	44.8
Range	18–70
Sex	
Male	11
Female	16
Localization tumor	
Extra-abdominal	14
Intra-abdominal	13
Tumor size	
< 5 cm	17
≥ 5 cm	8
NA	2
Treatment	
Excision and FU	23
Systemic	4
History	
Not relevant	19
Relevant	6
FAP syndrome	2
Mutation	
WT	10
Mutated	16
NI	1
Total number	27

NA not applicable, *FU* follow-up, *FAP* familial adenomatous polyposis, *NI* not informative

intra-abdominal surgery, including gastric bypass, whipple surgery and liver transplantation. For the extra-abdominal DTs, five were located on the proximal arm and shoulder, three on the proximal leg and two on the breast. Both breast tumors occurred after operation in this region, one after a breast prosthesis and one after breast amputation. The rest of the DTs were in different locations. All but one of the extra-abdominal tumors were located in the subcutis or within the muscle and only one was cutaneous. Two patients were known to have FAP syndrome. The diagnosis of all the tumors was confirmed histologically by morphology and by IHC for the beta-catenin antibody. Also, molecular analysis was performed. The materials were all examined for mutations on exon 3 of the CTNNB1 gene. One sample was not informative. Of the informative samples, almost 60% of the patients had the mutation, while 40% were wild type. IHC showed at least focal nuclear positivity of beta-catenin in the tumor cells, confirming the diagnosis in all cases, and also those with negative molecular results.

Immune composition of the tumor samples

Of all 33 samples, 24 came from excision specimens and 9 from biopsies. The tumor itself displayed no remarkable inflammatory infiltrate. According to our observation, a less described although constant finding in DTs is the presence of a lymphoid infiltrate in the form of lymphoid aggregates, usually at the periphery of the tumor adjacent to the surrounding tissue. Those lymphoid aggregates, defined as a group of 50 or more inflammatory cells [13], are mostly seen in the immediate proximity with small- to medium-sized blood vessels and it usually spreads in the tissue between adjacent vessels (Fig. 2). In our cases, we found such an inflammatory response at the periphery of the tumor in 88% of tumor specimens in the form of small lymphoid aggregates. The presence of germinal centers within the lymphoid aggregates was noted in two of our samples.

B cell marker CD20 was present in almost 86% of the specimens. There was a remarkable contrast between CD20 expression in lymphoid aggregates and stromal lymphocytes (Fig. 2). Those 86% of the cases showed at least moderate CD20 positivity in the lymphoid aggregates. On the other hand, in only 12% of the cases, stromal lymphocytes demonstrated low CD20 (score 1) immune reactivity. All other samples showed no expression for CD20.

T cell marker CD3 was found in all samples, on lymphocytes in the aggregates as well as in the stroma. Although CD4 and CD8 were almost equally strongly expressed on lymphocytes in the lymphoid aggregates (Fig. 2), this was not the case for stromal lymphocytes (Fig. 3) (Table 2). The majority of samples (73%) had no $CD4^+$ stromal lymphocytes, while another 97% of samples did display $CD8^+$ stromal lymphocytes. Regulatory T cells, identified by $CD4^+FoxP3^+$ cells, were seen in 83% of the lymphoid aggregates, while no $CD4^+FoxP3^+$ cells were found in the stromal lymphocytes.

CD45RO, a marker for effector and memory T cells, was expressed on the lymphocytes of the lymphoid aggregates in all our samples (Fig. 2) and on the stromal lymphocytes in nearly all of the samples (Fig. 3) (Table 2). Regarding the lymphoid aggregates, CD45RO was strongly present (score 4) in almost 93% and moderately present (score 3) in the rest of the cases. In the stroma, the CD45RO scores were distributed between low to strong expression.

A significant positive correlation between CD8 and CD45RO expression ($p = 0.009$, $R^2 = 0.448$) could be found in the stroma, while there was a negative correlation between CD8 and CD4 expression ($p = 0.000015$, $R^2 = -0.678$) in the stroma. This may indicate that the TILs in the stroma are $CD8^+$ memory T cells. We have also found a strong correlation between CD4 and CD45RO expression in the lymphoid aggregates ($p = 0.056$, $R^2 = 0.358$) which suggests the presence of $CD4^+$ memory T cells.

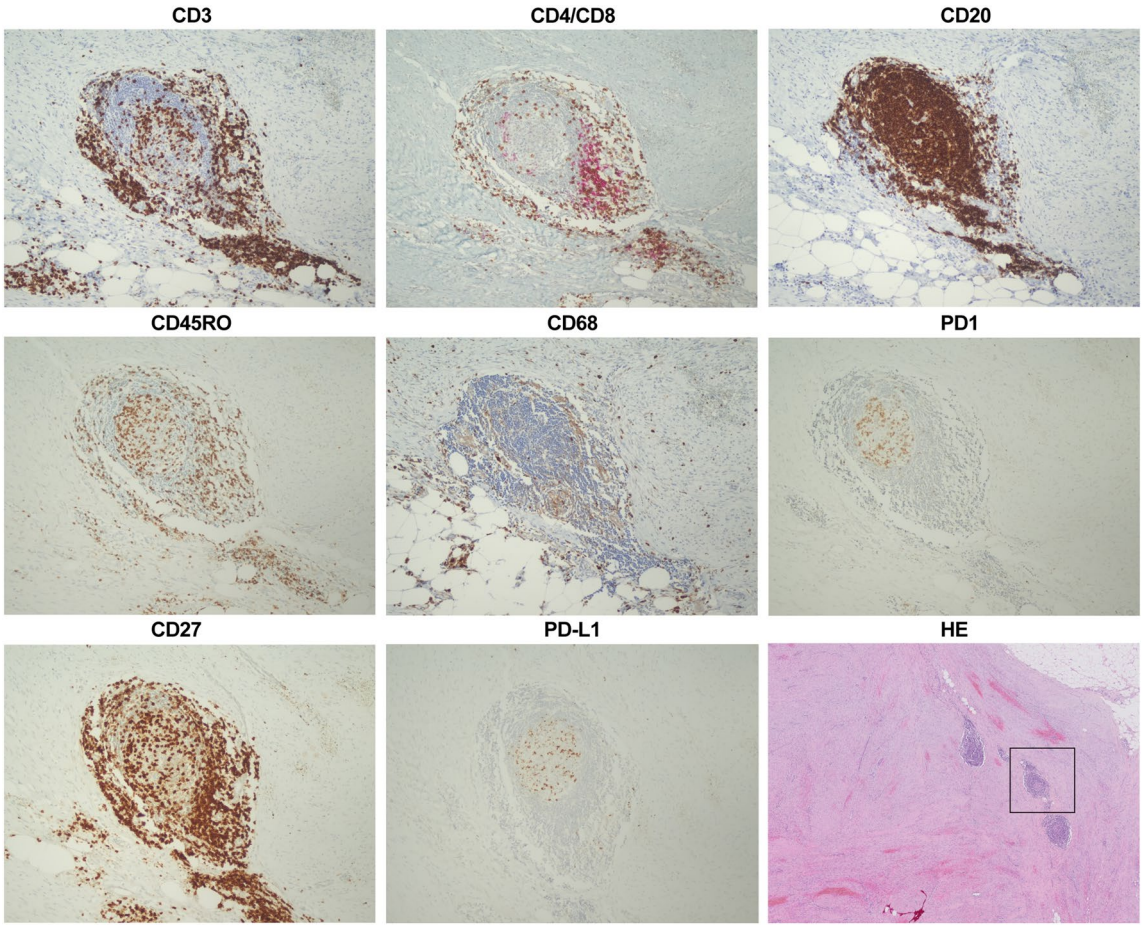

Fig. 2 Immune composition of a representative lymphoid aggregate at the periphery of the tumor. Dual staining was used for CD4 (red, cytoplasmic)/CD8 (brown, cytoplasmic). All tissue sections for immunohistochemistry were counterstained with hematoxylin (blue color). Original magnification ×200. An overview picture of the hematoxylin/eosin (HE) staining is depicted on the right, below. Original magnification ×50

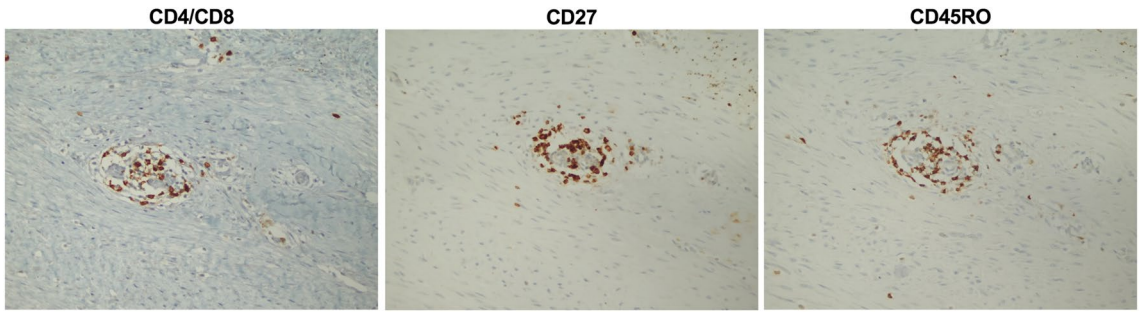

Fig. 3 Immune composition of the lymphocytic infiltrate in the tumoral stroma. Dual staining was used for CD4 (red, cytoplasmic)/CD8 (brown, cytoplasmic). No CD4 positivity could be detected in the tumoral stroma. All tissue sections were counterstained with hematoxylin (blue color). Original magnification ×200

Although no $CD68^+$ cells were found in the stroma, almost all samples (97%) showed CD68 expression in lymphoid aggregates (Fig. 2). The morphology of those $CD68^+$ cells was consistent with those of histiocytes. A significant correlation between CD68 and $CD4^+/FoxP3^+$ cells was encountered ($p = 0.038$, $R^2 = 0.386$) in the lymphoid aggregates.

Table 2 Expression of immune checkpoints and immune cell markers in desmoid tumors

N, % samples	CD3	CD20	CD4	CD4/FOXP3	CD8	CD56	CD45Ro	NKp46	CD68	Granzyme	CD27	CD70	PD1	PD-L1
Total ($n=33$)	33 (100%)	25 (86.2%)	29 (87.9%)	24 (72.7%)	32 (97%)	15 (45.5%)	33 (100%)	4 (12.1%)	28 (84.8%)	13 (39.4%)	28 (84.8%)	15 (45.5%)	27 (81.8%)	15 (45.5%)
Tumor cells ($n=33$)	0 (0%)	0 (0%)	0 (0%)	0 (0%)	0 (0%)	0 (0%)	0 (0%)	0 (0%)	0 (0%)	0 (0%)	0 (0%)	0 (0%)	13 (39.4%)	2 (6.1%)
Immune cells in stroma ($n=33$)	33 (100%)	4 (12.1%)	9 (27.3%)	0 (0%)	32 (97%)	3 (9.1%)	33 (100%)	0 (0%)	0 (0%)	0 (0%)	20 (60.6%)	1 (3%)	10 (30.3%)	0 (0%)
Lymphocytes in lymphoid aggregates ($n=29$)	29 (100%)	25 (86.2%)	29 (100%)	24 (82.6%)	29 (100%)	14 (48.3%)	29 (100%)	4 (13.8%)	28 (96.6%)	13 (44.8%)	27 (93.1%)	15 (51.7%)	24 (82.6%)	14 (48.3%)

Natural killer (NK) cells were not remarkably present in our samples. This was shown both with CD56, a homophilic binding glycoprotein whose expression is strongly associated with NK cells, and with NKp46. NKp46, a killer activation receptor expressed on the plasmatic membrane of NK cells, was not expressed on stromal lymphocytes and only low (score 1) expression was demonstrated in 14% of the aggregates. CD56 showed similar results with only one case showing mild expression of CD56 in the aggregates. Comparable results could be demonstrated for granzyme B, a protease expressed in the granules of different type of cells as cytotoxic lymphocytes and NK cells. There was no positivity for granzyme B in the stroma and only scattered positive cells could be observed in the aggregates.

Immune checkpoint expression

CD27, a TNF receptor superfamily member, was also a very important component of the lymphocytes, mainly those present in the lymphoid aggregates (Fig. 2): 93% of the samples had CD27-positive aggregates (Table 2). Interestingly, 39% of the cases had no $CD27^+$ stromal lymphocytes (Fig. 3). CD70 is a ligand for CD27 and is transiently expressed on activated lymphocytes. In our samples, CD70 was mild to moderately positive (score 2 and 3) in almost 52% of the aggregates, while it was absent in the stromal lymphocytes in all but one case. Moreover, no expression of CD70 on the tumor cells was seen. CD70 positivity in the lymphoid aggregates was strongly correlated with CD68 ($p=0.032$, $R^2=0.400$), CD20 ($p=0.009$, $R^2=0.475$) and granzyme ($p=0.021$, $R^2=0.467$). On the other hand, CD27 in the tumoral stroma was correlated with CD45RO ($p=0.008$, $R^2=0.457$) and CD20 ($p=0.082$, $R^2=0.308$).

The expression of the immune checkpoint PD1 and its ligand PD-L1 was evaluated both in the lymphocytes and in tumor cells. PD1 showed expression in the lymphoid aggregates (Fig. 2), but rather within the lower scores; no positivity within score 4 was seen. In the tumoral stroma, only 1 out of the 33 cases exhibited mild positivity (score 2), while the rest were negative or very lowly expressed (score 1). Interestingly enough, 40% of the tumor cells were also positive (33%, mainly score 2). All of the samples with lymphocytes in the stroma as well as half of the samples with lymphoid aggregates were negative for PD-L1. Tumor cells did also not express PD-L1 in 94% of the cases, while one case displayed score 1 and another one score 3. We found a strong correlation between PD1 and CD70 expression in het lymphoid aggregates ($p=0.015$, $R^2=0.448$). Finally, a correlation could be found between PDL1 positivity in the tumor cells and CD27 expression in the tumoral stroma ($p=0.030$, $R^2=0.379$).

Mutation analysis

PCR analysis was performed on all samples. Nineteen samples from 16 patients were mutated. Next-generation sequencing (NGS) analysis showed beta-catenin missense mutations in codons 41 and 45 of exon 3 (identified as c.121 A4G or pThr-41-Ala (T41A), c.133T4C or pSer45Pro (S45P), and c.134C4T or pSer45Phe (S45F)). The T41A mutation was the most common, occurring in 52% of the mutated samples, whereas the S45P and S45F mutations occurred in 16% of the same samples. The other samples were not informative for the NGS. We have identified a significant association between the extent of the lymphocytic infiltrate in the stroma and the mutation status. It was seen that patients with the S45F mutation were lacking an immune infiltrate in the stroma ($p=0.052$). Moreover, all mutated samples ($n=16$), independently of the codon that was involved, showed a very low PD-L1 expression in lymphoid aggregates ($p=0.022$).

Clinicopathological parameters

Within the clinical parameters, the one which is mostly correlated with the immune profile of the lesions is the tumor size. Bigger lesions contain a higher percentage cytotoxic T cells in the lymphoid aggregates, matching with score 4 ($p<0.001$). On the other hand, smaller tumors contain a higher percentage of lymphocytes ($p=0.022$). Additionally, smaller tumors demonstrate more $PD1^+$ lymphocytes in the aggregates ($p=0.015$), as well as more B cells (indicated by IHC for CD20) ($p=0.036$).

Discussion

We report a comprehensive study of the TME in DTs. To our knowledge, we are the first to characterize the immune microenvironment in DTs and to investigate the immune checkpoint expression in these tumors. Thereby, we are the first to demonstrate the presence of $CD4^+$ regulatory T cells in the lymphoid aggregates, while in the stroma a predominance of $CD8^+$ memory T cells could be noted. Moreover, we showed that although almost no PD-L1 was seen in the lymphocytes and in the tumor cells, PD1 was clearly present in both these cell types.

Several categories of immune cells can be found in a tumor and they can be located in the center, in the invasive margin or in the adjacent tertiary lymphoid organs (TLOs).

The majority of our samples showed an inflammatory response relying mainly on lymphocytes. In more than 85% of the samples, lymphoid aggregates were seen mainly localized around small- to medium-sized blood vessels at the tumor invasive margin in association with the surrounding normal tissue. Almost 86% of the samples with lymphoid aggregates showed high expression of CD20 (located on the surface of B cells) in the aggregates. T cells, marked by the expression of CD3, were also abundantly present in the lymphoid structures. It is well known that normal lymphoid structures, such as lymph nodes (LN), and other lymphoid organs, such as Payer's patches, are also composed of B and T cells that are required for defense against pathogens. Those structures are known as secondary lymphoid organs (SLO). The organization of lymphoid tissue with B and T lymphocytes around specialized blood vessels, as we also describe in our samples, mimics the SLOs and represents the TLOs or ectopic lymphoid tissue. Those blood vessels in the TLOs are specialized high endothelial venules (HEV) [14]. They seem to play a significant prognostic role in studies for breast carcinoma and melanoma, where the density of HEVs alone predicted patients outcome [15, 16]. TLOs are formed to mimic the SLOs at the lesion border, initiating the recruitment of hematopoietic cells through a complex procedure involving a chemokine-directed positive feedback loop [17, 18] and drive adaptive, antigen-specific immune response [17]. Those TLOs attract naive B and T cells which eventually will evolve into memory B and T cells after antigen proceeding. The lymphoid aggregates in our samples have a composition that highly relate to TLOs. Moreover, all those lymphoid structures in our material contained a high percentage of $CD45RO^+$ cells. The strong associations that we found between CD4 and CD45RO suggest the presence of CD4 memory T cells in the lymphoid aggregates. However, to confirm the presence of TLOs in our DT samples, further characterization is needed because apart from B and T cells, TLOs are further composed of mature dendritic cells (DCs). Especially, the presence of mature DCs in the intratumoral lymphoid structures was proven to be a better predictor of clinical outcome in patients with non-small cell lung cancer [19, 20].

The development and function of regulatory T cells (Tregs) depend on the transcription factor FoxP3. Naïve $CD4^+$ T cells convert into Tregs after transcription of FoxP3 [21]. In our series, a subset of $CD4^+$ T cells was also positive for FoxP3 in the lymphoid aggregates. Those double CD4- and FoxP3-positive lymphocytes in the aggregates suggest the presence of Tregs that are known for their pivotal role in maintaining immunologic tolerance [22]. Moreover, we found a strong association between the presence of Tregs and macrophages, marked by CD68, in the lymphoid structures. The presence of macrophages in the tumor microenvironment and their association with Tregs has been investigated the past years. Macrophages are known for their plasticity. In the tumor environment, they have the ability to transform to tumor-associated macrophages (TAMs) that enhance tumor progression [23, 24]. By secreting chemokine CCL22, Tregs are attracted in the tumor environment [23, 25, 26]. This

interaction could very well explain the significant association between $CD4^+FoxP3^+$ cells and $CD68^+$ cells that we found in our samples.

Signaling of CD27, a TNF receptor superfamily member, increases T cell expansion and function and is of importance in the maintenance of T cell memory [27–29]. Ruprecht and coworkers showed that in synovial fluid from patients with juvenile idiopathic arthritis, CD27 can also be used to as a marker for Tregs and can differentiate Tregs from activated effector T cells (Teff) [30, 31]. Furthermore, Duggleby et al. [32] described that for freshly isolated Tregs, only CD27 expression correlates with regulatory activity and could be used to isolate cells with regulatory activity from $CD4^+$ $CD25^+$ cells. Also, cells expressing high levels of FoxP3 were confined to the $CD27^+$ population. Within our research, we also could demonstrate that the $CD4^+FoxP3^+$ cells in the lymphoid aggregates were strongly correlated with CD27 expression in those aggregates, emphasizing the high probability that the observed $CD4^+FoxP3^+$ cells are indeed the Tregs.

Different observations regarding the immune cell composition were made for the tumoral stroma compared to the lymphoid aggregates. No B cells were found in the stroma and most of the $CD3^+$ cells here were $CD8^+$ T cells. Nevertheless, there was a significant association between the presence of $CD3^+$, $CD8^+$ and $CD45RO^+$ cells in the stroma, which implies the presence of $CD8^+$ memory T cells in the stroma. The role of cytotoxic memory T cells in tumors has been a great subject of investigation over the recent years. The main research was done on colorectal cancer where Bernard Mlecnik et al. [33] showed in 2011 that the density of $CD8^+$ memory cells was associated with low rates of tumor recurrence and that the assessment of $CD8^+$ memory T cells in combined tumor regions provides an indicator of tumor recurrence beyond that predicted by AJCC/UICC-TNM staging. It seems that $CD8^+$ memory T cells have a more direct role in killing the cancer cells, while $CD4^+$ T helper cells function in a more complicated way [34]. Naïve CD4 T cells differentiate into T helper type 1 (T_H1) cells and produce interferon gamma, which promotes CD8 T cell-mediated adaptive immunity [35]. Many other studies on different tumor types underscored the participation of CD45RO memory T cells as crucially important for favorable patient outcome [20, 33–40]. Further research is needed to establish the prognostic value of stromal $CD8^+$ memory T cells in the DTs.

In our samples, there was only limited CD56 positivity in both the lymphoid aggregates and the stroma, while NKp46 staining was absent. NKp46 receptor is considered to be the major lysis receptor for NK cells, capable of mediating direct killing of virus-infected cells and tumor cells [41]. The absence of NKp46 might be explained by the fact that NK cells are not attracted to being infiltrated in the tumor through inactivation of their receptor ligands or through secretion of immunosuppressive molecules [42].

Tumor size was significantly correlated with the expression of both CD8 and PD1 in the lymphoid aggregates. Interestingly, those two parameters were negatively correlated with each other and with the tumor size. As such, this suggests that lymphoid aggregates of bigger tumors contain more $CD8^+$ T cells and less PD1 positivity. Although the presence of CD8 cytotoxic cells in the tumoral stroma has been negatively correlated with the tumor size in patients with breast carcinoma [43], we found that larger tumors contain more CD8 cytotoxic lymphocytes. However, in our cases it concerns CD8 cytotoxic lymphocytes in the lymphoid aggregates at the periphery of the tumors and not in the tumoral stroma. In the cancer–immunity cycle [44], it is described that for the T cells to kill the cancer cells, T cells should recognize the cancer cells. This could in our cases explain why although there are CD8 cells in the lymphoid aggregates, the tumor continues to grow. It is possibly because those immune cells do not recognize the tumor antigens. PD1 is known to be a marker of exhausted $CD8^+$ cells [45]. In our cases, $CD8^+$ cells do not show PD1 expression, suggesting that they do not have an exhausted phenotype.

Another feature we observed in the tumors we investigated is the correlation of CD45RO with CD27 in the tumoral stroma and PD-L1 in the tumor cells. This may imply that the PD-L1 expression in the tumor cells is associated with the presence of memory T cells.

Lazar et al. [3] described that the S45F mutation is a prognostic factor strongly associated with recurrence in patients suffering from DTs. We found that all patients with mutations of the codon 45, mainly the S45F mutation, show almost no or very limited lymphocytic infiltrate in the tumor. Although our sample size is rather limited, this finding correlates with the results of Lazar et al. A low number of lymphocytes in the tumor microenvironment indicate limited antitumor defense, which may indirectly explain the greater incidence of recurrence in tumors with this mutation.

To conclude, we are the first to describe the immune composition in DTs. We showed the presence of lymphoid structures at the periphery of the tumor, strongly resembling TLOs that serve as ectopic lymphoid tissue, helping in recruitment of lymphoid cells at the tumor. Moreover, we demonstrated the presence of memory T cells both in the lymphoid aggregates and in the tumoral stroma. The lymphoid aggregates contain also a significant number of Tregs. However, while immune cells are clearly present in the lymphoid aggregates, a strong stromal antitumor immune response is lacking. There was no PD-L1 expression on tumor cells, and PD1 was partially expressed in the lymphoid aggregates but very limited in the tumoral stroma, which means that DTs are possibly not the best candidates for immune checkpoint blockade. Thus, we conclude that

further research into other immunotherapeutic targets for DTs is needed to trigger the immune system.

Acknowledgements The majority of human biological material used in this publication was provided by the Tumor bank, Antwerp University Hospital, Belgium, which is funded by the National Cancer Plan.

Author contributions VS, EM and JJ designed the study and performed the data acquisition and analysis. CH processed the slides. KZ and SP performed the immunohistochemical staining. CH provided patient material. All authors contributed to the interpretation of the data, sample collection, drafting and revision of the manuscript.

Funding The authors received no specific funding for this work.

Compliance with ethical standards

Conflict of interest All authors declare that they have no conflicts of interest.

Ethical approval and ethical standards We received approval by the Ethics Committee of the Antwerp University Hospital/University of Antwerp (EC 18/45/517) to use historical samples. As it was a retrospective study, no informed consent of the patients could be obtained.

References

1. Rizvi NA, Mazieres J, Planchard D et al (2015) Activity and safety of nivolumab, an anti-PD-1 immune checkpoint inhibitor, for patients with advanced, refractory squamous non-small-cell lung cancer (CheckMate 063): a phase 2, single-arm trial. Lancet Oncol 16:257–265. https://doi.org/10.1016/S1470-2045(15)70054-9
2. Escobar C, Munker R, Thomas JO, Li BD, Burton GV (2012) Update on desmoid tumors. Ann Oncol 23:562–569. https://doi.org/10.1093/annonc/mdr386
3. Lazar AJ, Tuvin D, Hajibashi S et al (2008) Specific mutations in the beta-catenin gene (CTNNB1) correlate with local recurrence in sporadic desmoid tumors. Am J Pathol 173:1518–1527. https://doi.org/10.2353/ajpath.2008.080475
4. Gurbuz AK, Giardiello FM, Petersen GM, Krush AJ, Offerhaus GJ, Booker SV, Kerr MC, Hamilton SR (1994) Desmoid tumours in familial adenomatous polyposis. Gut 35:377–381
5. Calvert GT, Monument MJ, Burt RW, Jones KB, Randall RL (2012) Extra-abdominal desmoid tumors associated with familial adenomatous polyposis. Sarcoma 2012:726537. https://doi.org/10.1155/2012/726537
6. Carlson JW, Fletcher CD (2007) Immunohistochemistry for beta-catenin in the differential diagnosis of spindle cell lesions: analysis of a series and review of the literature. Histopathology 51:509–514. https://doi.org/10.1111/j.1365-2559.2007.02794.x
7. Kasper B, Strobel P, Hohenberger P (2011) Desmoid tumors: clinical features and treatment options for advanced disease. Oncologist 16:682–693. https://doi.org/10.1634/theoncologist.2010-0281
8. Kasper B, Baumgarten C, Bonvalot S et al (2015) Management of sporadic desmoid-type fibromatosis: a European consensus approach based on patients' and professionals' expertise—a sarcoma patients EuroNet and European organisation for research and treatment of cancer/soft tissue and bone sarcoma group initiative. Eur J Cancer 51:127–136. https://doi.org/10.1016/j.ejca.2014.11.005
9. Mahoney KM, Rennert PD, Freeman GJ (2015) Combination cancer immunotherapy and new immunomodulatory targets. Nat Rev Drug Discov 14:561–584. https://doi.org/10.1038/nrd4591
10. Sharma P, Allison JP (2015) The future of immune checkpoint therapy. Science 348:56–61. https://doi.org/10.1126/science.aaa8172
11. Burgess M, Tawbi H (2015) Immunotherapeutic approaches to sarcoma. Curr Treat Options Oncol 16:26. https://doi.org/10.1007/s11864-015-0345-5
12. Jacobs J, Zwaenepoel K, Rolfo C et al (2015) Unlocking the potential of CD70 as a novel immunotherapeutic target for non-small cell lung cancer. Oncotarget 6:13462–13475. https://doi.org/10.18632/oncotarget.3880
13. Marcq E, Siozopoulou V, De Waele J et al (2017) Prognostic and predictive aspects of the tumor immune microenvironment and immune checkpoints in malignant pleural mesothelioma. Oncoimmunology 6:e1261241. https://doi.org/10.1080/2162402X.2016.1261241
14. Ager A (2017) High endothelial venules and other blood vessels: critical regulators of lymphoid organ development and function. Front Immunol 8:45. https://doi.org/10.3389/fimmu.2017.00045
15. Martinet L, Le Guellec S, Filleron T, Lamant L, Meyer N, Rochaix P, Garrido I, Girard JP (2012) High endothelial venules (HEVs) in human melanoma lesions: major gateways for tumor-infiltrating lymphocytes. Oncoimmunology 1:829–839. https://doi.org/10.4161/onci.20492
16. Martinet L, Garrido I, Filleron T, Le Guellec S, Bellard E, Fournie JJ, Rochaix P, Girard JP (2011) Human solid tumors contain high endothelial venules: association with T- and B-lymphocyte infiltration and favorable prognosis in breast cancer. Cancer Res 71:5678–5687. https://doi.org/10.1158/0008-5472.CAN-11-0431
17. Jones GW, Hill DG, Jones SA (2016) Understanding immune cells in tertiary lymphoid organ development: it is all starting to come together. Front Immunol 7:401. https://doi.org/10.3389/fimmu.2016.00401
18. Jing F, Choi EY (2016) Potential of cells and cytokines/chemokines to regulate tertiary lymphoid structures in human diseases. Immune Netw 16:271–280. https://doi.org/10.4110/in.2016.16.5.271
19. Dieu-Nosjean MC, Antoine M, Danel C et al (2008) Long-term survival for patients with non-small-cell lung cancer with intratumoral lymphoid structures. J Clin Oncol 26:4410–4417. https://doi.org/10.1200/JCO.2007.15.0284
20. Pages F, Galon J, Dieu-Nosjean MC, Tartour E, Sautes-Fridman C, Fridman WH (2010) Immune infiltration in human tumors: a prognostic factor that should not be ignored. Oncogene 29:1093–1102. https://doi.org/10.1038/onc.2009.416
21. Hori S, Nomura T, Sakaguchi S (2003) Control of regulatory T cell development by the transcription factor Foxp3. Science 299:1057–1061. https://doi.org/10.1126/science.1079490
22. Hinz S, Pagerols-Raluy L, Oberg HH et al (2007) Foxp3 expression in pancreatic carcinoma cells as a novel mechanism of immune evasion in cancer. Cancer Res 67:8344–8350. https://doi.org/10.1158/0008-5472.CAN-06-3304
23. Chanmee T, Ontong P, Konno K, Itano N (2014) Tumor-associated macrophages as major players in the tumor microenvironment. Cancers (Basel) 6:1670–1690. https://doi.org/10.3390/cancers6031670
24. Jinushi M, Komohara Y (2015) Tumor-associated macrophages as an emerging target against tumors: creating a new path from bench to bedside. Biochim Biophys Acta 1855:123–130. https://doi.org/10.1016/j.bbcan.2015.01.002
25. Curiel TJ, Coukos G, Zou L et al (2004) Specific recruitment of regulatory T cells in ovarian carcinoma fosters immune privilege and predicts reduced survival. Nat Med 10:942–949. https://doi.org/10.1038/nm1093

26. Mizukami Y, Kono K, Kawaguchi Y, Akaike H, Kamimura K, Sugai H, Fujii H (2008) CCL17 and CCL22 chemokines within tumor microenvironment are related to accumulation of Foxp3 + regulatory T cells in gastric cancer. Int J Cancer 122:2286–2293. https://doi.org/10.1002/ijc.23392
27. Matter M, Mumprecht S, Pinschewer DD, Pavelic V, Yagita H, Krautwald S, Borst J, Ochsenbein AF (2005) Virus-induced polyclonal B cell activation improves protective CTL memory via retained CD27 expression on memory CTL. Eur J Immunol 35:3229–3239. https://doi.org/10.1002/eji.200535179
28. Claus C, Riether C, Schurch C, Matter MS, Hilmenyuk T, Ochsenbein AF (2012) CD27 signaling increases the frequency of regulatory T cells and promotes tumor growth. Cancer Res 72:3664–3676. https://doi.org/10.1158/0008-5472.CAN-11-2791
29. Matter MS, Claus C, Ochsenbein AF (2008) CD4 + T cell help improves CD8 + T cell memory by retained CD27 expression. Eur J Immunol 38:1847–1856. https://doi.org/10.1002/eji.200737824
30. Jiang Y, Li Y, Zhu B (2015) T-cell exhaustion in the tumor microenvironment. Cell Death Dis 6:e1792. https://doi.org/10.1038/cddis.2015.162
31. Ruprecht CR, Gattorno M, Ferlito F, Gregorio A, Martini A, Lanzavecchia A, Sallusto F (2005) Coexpression of CD25 and CD27 identifies FoxP3 + regulatory T cells in inflamed synovia. J Exp Med 201:1793–1803. https://doi.org/10.1084/jem.20050085
32. Duggleby RC, Shaw TN, Jarvis LB, Kaur G, Gaston JS (2007) CD27 expression discriminates between regulatory and non-regulatory cells after expansion of human peripheral blood CD4 + CD25 + cells. Immunology 121:129–139. https://doi.org/10.1111/j.1365-2567.2006.02550.x
33. Mlecnik B, Tosolini M, Kirilovsky A et al (2011) Histopathologic-based prognostic factors of colorectal cancers are associated with the state of the local immune reaction. J Clin Oncol 29:610–618. https://doi.org/10.1200/JCO.2010.30.5425
34. Hadrup S, Donia M, Thor Straten P (2013) Effector CD4 and CD8 T cells and their role in the tumor microenvironment. Cancer Microenviron 6:123–133. https://doi.org/10.1007/s12307-012-0127-6
35. Galon J, Costes A, Sanchez-Cabo F et al (2006) Type, density, and location of immune cells within human colorectal tumors predict clinical outcome. Science 313:1960–1964. https://doi.org/10.1126/science.1129139
36. Galon J, Pages F, Marincola FM, Thurin M, Trinchieri G, Fox BA, Gajewski TF, Ascierto PA (2012) The immune score as a new possible approach for the classification of cancer. J Transl Med 10:1. https://doi.org/10.1186/1479-5876-10-1
37. Fridman WH, Pages F, Sautes-Fridman C, Galon J (2012) The immune contexture in human tumours: impact on clinical outcome. Nat Rev Cancer 12:298–306. https://doi.org/10.1038/nrc3245
38. Giraldo NA, Becht E, Pages F et al (2015) Orchestration and prognostic significance of immune checkpoints in the microenvironment of primary and metastatic renal cell cancer. Clin Cancer Res 21:3031–3040. https://doi.org/10.1158/1078-0432.CCR-14-2926
39. Appay V, van Lier RA, Sallusto F, Roederer M (2008) Phenotype and function of human T lymphocyte subsets: consensus and issues. Cytometry A 73:975–983. https://doi.org/10.1002/cyto.a.20643
40. Donnem T, Hald SM, Paulsen EE et al (2015) Stromal CD8 + T-cell density-A promising supplement to TNM staging in non-small cell lung cancer. Clin Cancer Res 21:2635–2643. https://doi.org/10.1158/1078-0432.CCR-14-1905
41. Mandelboim O, Porgador A (2001) NKp46. Int J Biochem Cell Biol 33:1147–1150
42. Prendergast GC, Jaffee EM (2013) Cancer immunotherapy: immune suppression and tumor growth, 2nd edition. Elsevier/AP, Academic Press is an imprint of Elsevier, Amsterdam; Boston
43. Riazi Rad F, Ajdary S, Omranipour R, Alimohammadian MH, Hassan ZM (2015) Comparative analysis of CD4 + and CD8 + T cells in tumor tissues, lymph nodes and the peripheral blood from patients with breast cancer. Iran Biomed J 19:35–44
44. Chen DS, Mellman I (2013) Oncology meets immunology: the cancer-immunity cycle. Immunity 39:1–10. https://doi.org/10.1016/j.immuni.2013.07.012
45. Lee J, Ahn E, Kissick HT, Ahmed R (2015) Reinvigorating exhausted T cells by blockade of the PD-1 pathway. For Immunopathol Dis Therap 6:7–17. https://doi.org/10.1615/ForumImmunDisTher.2015014188